ELECTROMAGNETIC PROPERTIES OF SELECTED HEXAFERRITES

A. Grusková[1], J. Sláma[1], A. González[2], V. Ďurman[1], M. Ušáková[1], V. Jančárik[1], M. Šoka[1]

[1]*Slovak University of Technology, Faculty of Electrical Engineering and Information Technology, Ilkovičova 3, 81219 Bratislava, Slovak Republic*
[2]*Facultad de Ingenieria, Universidad Autónoma de Baja California, Blvd. Benito Juárez s/n, Cp 21280 Mexicali, B. C., México*

Summary $Ba(Sr)(Me_1^{2+}Me_2^{4+})_xFe_{12-x}O_{19}$ hexagonal ferrites preparation with substitution ratio of $0.0 \le x \le 0.6$. The iron ions were substituted by selected cation combinations (divalent Me_1^{2+} = Ni, Zn, Sn, Co and tetravalent Me_2^{4+}= Ti, Zr, Ru ions). The samples were synthesised by high energy milling and metallorganic precursor method. A special attention was focused to results obtained for $(ZnTi)_x$ substitutions. The changes of coercivity H_C were chosen as a evaluation criterion of anisotropy variation. Simultaneously with the magnetic properties, the dielectric parameters were also tested. Two dielectric relaxation processes were detected in Ba - Sr ferrite. Our results showed probably a ferroelectric behaviour of some ferrite samples.

1. INTRODUCTION

M-type hexaferrite $BaFe_{12}O_{19}$ (BaM) is one of the most important hard magnetic materials widely used in many applications. For its high stability, excellent high-frequency response and narrow switching field distribution, BaM has been studied extensively during the last few years. Despite a considerable amount of published research over the past decade related to the substituted barium ferrites magnetic properties and microstructure, there have been only a few successful breakthroughs regarding the discovery of new compositions, with excellent properties for special applications.

A large amount of researches has been realized to modify the magnetic properties of barium hexaferrite by substitution of Fe^{3+} ions with other trivalent cations or divalent Me_1^{2+} and tetravalent Me_2^{4+} cation combinations and/or Ba^{2+} ion by other cations [1-10]. The magnetic properties of substituted ferrites depend directly of both electronic configuration and preference to occupy the non-equivalent Fe^{3+} sublattices of the substituted cations on hexagonal structure. Replacing Fe^{3+} ions by other less magnetic moment, paramagnetic or diamagnetic cations leads to changes in the exchange interactions between the magnetic sublattices and to the appearance of new positions of Fe^{3+} ions. It causes reduction of the high uniaxial anisotropy field of the Ba ferrite. In addition, substituted Ba hexaferrites are very promising materials as electronic wave absorbers, especially at frequencies up to 50 GHz [4].

In the present work, our attention was focused on the study of magnetic and dielectric properties of $Ba_{1-y}Sr_yFe_{12}O_{19}$ as part of M-type hexagonal ferrite general studies, where y = 0.00, 0.25, 0.50, 0.75 and 1.00. Moreover, Zn^{2+} and Ti^{4+} ions were mainly used as substitutions aiming to change the magnetic properties of $Ba_{0.5}Sr_{0.5}Fe_{12}O_{19}$ hexaferrite prepared by low temperature auto-combustion method [10]. Properties of $(BaSr)_{0.5}M(ZnTi)_x$ ferrites were compared with those substituted $Ba(Me_1Me_2)_xFe_{12-2x}O_{19}$ ferrites prepared by mechanical milling and metallorganic precursor methods. The Fe^{3+} ions were substituted by selected ion combinations, divalent Me_1^{2+} = Ni, Zn, Sn, Co together with tetravalent Me_2^{4+} = Ti, Zr, Ru cations.

2. MATERIAL PREPARATION

Samples of $Ba(Me_1Me_2)_xFe_{12-2x}O_{19}$ with divalent Me_1 =Ni, Sn, Zn and tetravalent Me_2 = Ti, Zr, Ru ion combinations were synthesised by high energy milling. The samples (assigned as Mx in the following text) were produced by mechanical milling using $BaCO_3$, Fe_2O_3 NiO, ZnO, SnO, SnO_2 and RuO_2 (all with purity of 98%). The mechanical milling was performed in a Segvari attritor using the ball/powder ratio of 15 and the Fe/Ba ratio of 10. The powders were milled within 28 hours in air with an angular velocity of 400 rpm and with 250 ml of benzene added to avoid agglomeration at bottom of mill. After mechanical milling, the samples were annealed at 1050°C for 1.5 hours.

Samples of $Ba(Me_1Me_2)_xFe_{12-2x}O_{19}$ with divalent Me_1 = Co, Zn and tetravalent Me_2 = Ti, Zr, ion combinations (assigned as Sk in the following text) were prepared using an metallorganic precursor. $Ba(OH)_2.8H_2O$, $Fe(NO_3)_3.9H_2O$ and other ions as soluble salts and citric acid, all of purity of 99%, were used as the starting materials. In this case a Fe/Ba ratio of 10.8 was used. The amorphous citrate precursor was decomposed at 360°C for 5 hours. The samples were subsequently annealed at temperatures 700°C and 1050°C for 1.5 hours.

3. METHODS OF CHARACTERIZATION

The phase purity of the samples was evaluated by the temperature dependence of initial susceptibility $\chi(T)$ and specific saturation polarization $J_{S\text{-}m}(T)$ [11]. They were measured by using the bridge method in an alternating magnetic field of 421 A/m and 920 Hz and by a vibrating sample magnetometer Lake Shore 430 VSM applying an external magnetic field up to 1.2 T. The structure of samples was analysed by the Mössbauer spectroscopy and the X-

ray diffraction. The measurements were performed by a Mössbauer spectrometer with γ-ray source of ^{57}Co imbibed in a rhodium matrix. For the diffraction measurements an X´ Pert Philips diffractometer was used with Cu-K_α radiation. The particle size and shape were observed by a Philips XL 30 scanning electron microscope (SEM).

Dielectric properties of substituted Ba ferrites were also investigated assuming that they could help to analyse the samples structure. The impedance measurements at room temperature were carried out by using HIOKI Z HiTESTER 3531 in the frequency range from 42 Hz to 2 MHz with measuring voltage of 1 V.

4. RESULTS AND DISCUSSION

The changes of coercivity H_C were chosen as evaluation criteria of anisotropy variation. The evolution of H_C with x can be expressed by the coercivity difference, $\Delta H_c(x)=H_c(x)-H_c(0)$, where $H_C(0)$ is the coercivity of sample with $x=0$. Thus $\Delta H_C(x)$ reflects the change of coercivity comparing with the pure BaM ferrite. The variation of ΔH_C as a function of substitution ratio x for selected samples prepared by mechanical milling method (Mx) is presented in Fig. 1. The changes of ΔH_C with x for the BaM(ZnTi), BaM(CoTi) and $(BaSr)_{0.5}$M(ZnTi) samples prepared by the precursor method (Sk) are shown in Fig. 2. They were compared with BaM(CoIr) samples (Mx) published in [12]. The experimental data in both Fig. 1 and Fig. 2 and also the data from our previous experiments [6 - 10] could be resolved as follows. The course of the uniaxial anisotropy of BaM hexaferrites when $2x$ Fe^{3+} cations are substituted by x Me_1^{2+} (Ni, Zn, Sn, Co) and x Me_2^{4+} (Ti, Zr) showed a decrease with x, but it is not entirely planar over the range of substitutions from x = 0 to 0.6 [6, 7]. The ordering temperature T_C and the specific saturation polarization $J_{s\text{-}m}$ were reduced with x. This behaviour restricts the performances in terms of the microwave absorption and the usable range of temperatures. For example, in the CoTi cation mixture the ΔH_C decreases relative slowly and its value becomes constant for x = 1.2 [6]. It is a consequence of the fact that the uniaxial anisotropy of BaM becomes planar for $x \cong 1.2$. Doping with $(CoIr)_x$ [12] produces also the change of anisotropy from axial to planar for the values of x smaller than 0.6 (Fig. 2). The specific saturation polarization increases with x but it presents a significant lower H_C level than $(CoTi)_x$ and $(ZnTi)_x$ mixtures. Besides, we have also found that replacing of Fe^{3+} in BaM with SnRu, NiSn and SnSn produces the similar decrease of uniaxial anisotropy for the values of x smaller than 0.6. For substitutions with $(SnRu)_x$, the ΔH_C decreasing tendency with x is shown in Fig. 1 as an example. The strong decrease of ΔH_C up to x = 0.3 for $(NiRu)_x$ [8] leads to conclusion that the anisotropy of $(NiRu)_x$ becomes planar at a small substitution level. We observed the same trend of uniaxial anisotropy in $(ZnRu)_x$ [8]. In addition, this tendency was observed also in the case of $(CoRu)_x$ substitution [4]. Structural refinements on $(NiRu)_x$ and $(ZnRu)_x$ substitutions have shown, that Ru^{4+} preferentially replaced the Fe^{3+} ions on 2b site for low x; and then octahedral sites $4f_2$ + 2a (for Zn as partner ion) or on tetrahedral sites $4f_1$ for Ni as partner ion (see Table 1). Therefore we attribute the rapid change of anisotropy and H_C in $(NiRu)_x$ and $(ZnRu)_x$ to preferential occupation of 2b site by Ru^{4+} ion. We observed, that not only Ru^{4+} ions, but also Me^{2+} (Ni, Zn, Co, Sn) ions have an influence on ΔH_C. However, their effect is much less significant. This opinion confirms the change of ΔH_C with x for ($Sn^{2+}Ru^{4+}$) substitution. SnRu produces a visible lower change of ΔH_C comparing with NiRu (or ZnRu) substitution for $x \leq 0.3$. In spite of that, Sn^{2+} probably occupies the same $4f_2$ and 2a sites in $Sn^{2+}Ru^{4+}$ as well as Ni^{2+} does in NiRu sample, while Ru^{4+} occupies the identical 2b and $4f_1$ sites in both mixtures. The different influence of divalent Ni (or Zn, Co) and Sn ions on the behaviour of ΔH_C as a function of x may be explained by the fact that Ni ($3d^8$) has only 3d orbitals structure like as Zn (diamagnetic) and Co, whereas divalent Sn (diamagnetic) has ($3d^{10}$, $4d^{10}$) orbital structure and also different electronic configuration. The both groups of ions Ni (or Zn, Co) and Sn replace the Fe^{3+} ($3d^5$) ions in the individual sites.

The magnetic susceptibility temperature dependences of the $Ba(ZnTi)_xFe_{12-2x}O_{19}$ and $(BaSr)_{0.5}(ZnTi)_xFe_{12-2x}O_{19}$ are shown in Fig. 3a and 3b. They can be used for quality tests and judging the convenience of sample preparation. From the values of $\chi(T)$ for x = 0.0 we can deduce, that no other secondary phase was nucleated in the specimens.

Tab 1. Ionic parameters and preference occupying sites of substituted mixtures

Substitution		Orbit	Radius	Electro-negativity	$4f_2$ octa	2a octa	$4f_1$ tetra	12k octa	2b hexa
Zn^{2+}–Ru^{4+}	Zn^{2+}	$3d^{10}$	0.074	1.65			*		
	Ru^{4+}	$4d^4$	0.067	2.20	*	*			*
Sn^{2+}–Ru^{4+}	Sn^{2+}	$4d^{10}$	0.112	1.96	*	*			
Ni^{2+}–Ru^{4+}	Ni^{2+}	$3d^8$	0.072	1.91	*	*			
	Ru^{4+}	$4d^4$	0.067	2.20			*		*
Lattice momentum (μ_B)					↓ –10	↑ +5	↓ –10	↑ +30	↑ +5

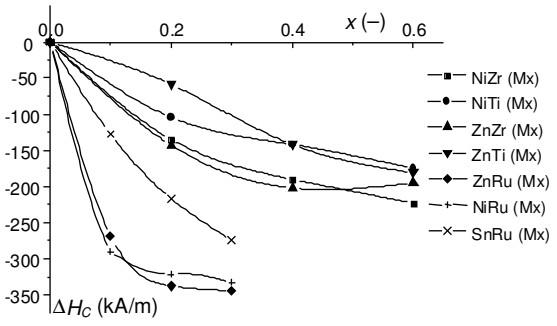

Fig. 1. Change of coercivity difference ΔH_C as a function of x for the samples prepared by mechanical milling

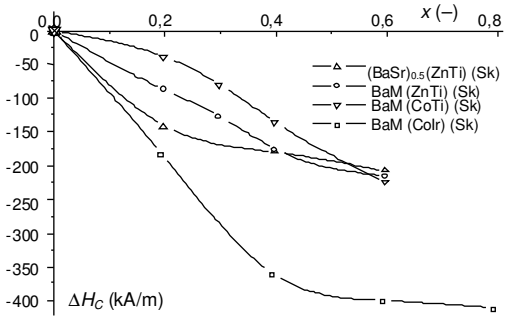

Fig. 2. Change of coercivity difference ΔH_C on x for the samples prepared by precursor method

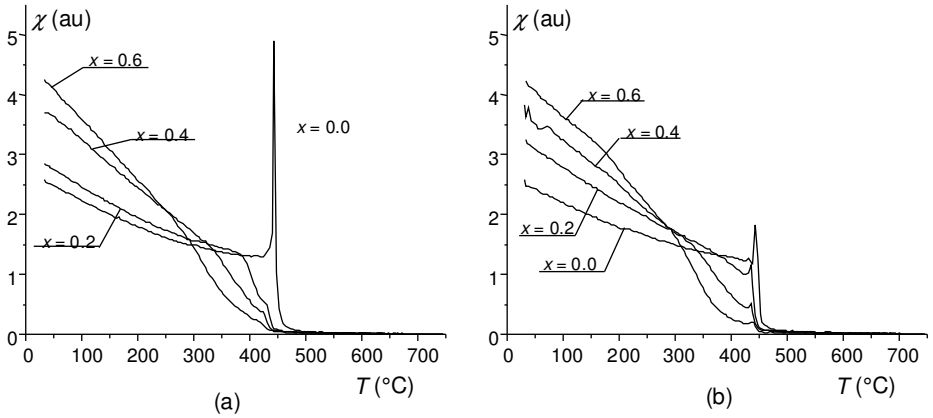

Fig. 3. Temperature dependence of magnetic susceptibility $\chi(T)$ of $Ba(ZnTi)_xFe_{12-2x}O_{19}$ (a) and $(BaSr)_{0.5}(ZnTi)_xFe_{12-2x}O_{19}$ (b)

The Hopkinson peak appears in the vicinity of the Curie point T_C. Behind the T_C the $\chi(T)$ curve falls from a relative high value to near zero. The slope of this drop gives the compositional chemical homogeneity measure of the sample. The peak value provides information about the percentage of the ordered single-phase structure with particles smaller than 1 μm. Samples with $x = 0.0$ exhibit a curve that roughly approaches to theoretical behaviour of the hexaferrite initial magnetic susceptibility. This fact is more evident for BaM ferrite in Fig. 3a. Since the drop of $\chi(T)$ at the T_C is almost vertical, the Curie temperature is practically the same within the volume of the samples. We can see that the Hopkinson peak is vanished with ZnTi substitutions, which may be connected with grain rising (Fig. 3a). In the sample $(BaSr)_{0.5}M$ (Fig. 3b), there is just a small indication of the Hopkinson´s peak. The particles are probably large and multi-domain. The substitution with $(ZnTi)_x$ provides a similar character of curves as for the $BaM(ZnTi)_x$ samples. Simply, it is difficult to estimate the phase homogeneity using $\chi(T)$ evaluation technique for the samples with $x = 0.4$ and 0.6 (Fig. 3a, b). As x decreases, the behaviour of susceptibility doesn't approach to the susceptibility of the sample with $x = 0.0$. The experimental data measured for $x > 0.0$ indicate that T_C is not uniform within the volume of the sample. On the other hand, it can be seen that T_C of some magnetic phases for all substituted samples were almost not affected by the increase in x, (diminution ~2%). It was also observed, that at room temperature the susceptibility χ increases with the substitution level. It is probably related to changes of the magneto-crystalline anisotropy of the samples. The $\chi(T)$ behaviour requires a more detailed analysis for all samples with substitution ratio $x \geq 0.2$.

The influence of $(ZnTi)_x$ substitution on the hysteresis loop of BaM and $(BaSr)_{0.5}M$ ferrites are shown in Fig. 4a and 4b. We can see an evident decrease of ΔH_C with x for both samples. It is similar to the decrease in Fig. 2b. There is a 19% drop of the specific remanent polarization $J_{s\text{-}r}$ with increasing x whereas the specific saturated polarization $J_{s\text{-}m}$ diminishes more slowly for both $BaM(ZnTi)_x$ and $(BaSr)_{0.5}M(ZnTi)_x$ ferrites. In the $(BaSr)_{0.5}M$ ferrite the value of H_C is 5.9% higher comparing with H_C in pure BaM ferrite. On the other hand the value of $J_{s\text{-}m}$ is of 5.4% higher in BaM ferrite.

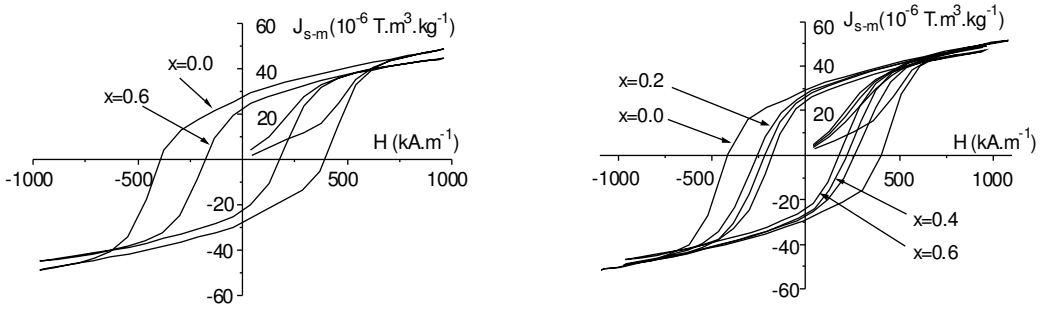

a) *b)*

Fig. 4 Hysteresis loops of $Ba(ZnTi)_xFe_{12-2x}O_{19}$ for x = 0.0 and 0.6 (a) and $(BaSr)_{0.5}(ZnTi)_xFe_{12-2x}O_{19}$ for x = 0.0, 0.2, 0.4, 0.6 (b)

The dielectric parameters of the ferrite samples measured by an impedance analyser were processed in the form of the complex permittivity $\varepsilon^*(f)$. The permittivity can be approximated by the locus diagram in the complex plane where the real part $\varepsilon'(f)$ of the complex permittivity is plotted against the imaginary component $\varepsilon''(f)$. The frequency dependence of ε^* for $Ba_{0.5}Sr_{0.5}Fe_{12}O_{19}$ ferrite is shown in Fig. 5 and the one for $Ba_{0.25}Sr_{0.75}Fe_{12}O_{19}$ is shown in Fig. 6.

The locus diagram $\varepsilon^*(f)$ in Fig. 5 indicates a presence of a relaxation effect. It can be expressed and fitted by the Cole-Cole relaxation formula

$$\varepsilon^*(f) = \varepsilon_\infty + \frac{\varepsilon_s - \varepsilon_\infty}{1+(j2\pi fT)^{1-\nu}}, \qquad (1)$$

where $\varepsilon_\infty \approx 20$ is the nonrelaxation permittivity, $\varepsilon_s \approx 595$ is the static permittivity, T is the relaxation time and ν is the material parameter.

The locus diagram $\varepsilon^*(f)$ shown in Fig. 6 is determined by two polarization processes. To resolve the low frequency behaviour, two points of spectra near $f \to 0$ Hz were approximated and added to the measured values. We suppose that the first polarization process is connected with relaxation and hysteresis effects at low frequencies. The second polarization process is probably based on a pure relaxation effect in the higher frequency region (from ≈ 28 kHz up to 2 MHz). The diagram $\varepsilon^*(f)$ is expressed by the relation

$$\varepsilon^*(f) = \begin{cases} \varepsilon_{\infty 1} + \dfrac{\varepsilon^*_{s1} - \varepsilon_{\infty 1}}{1+(j2\pi fT_1)^{1-\nu_1}} & 0 < f \le 4\,\text{kHz} \\ F(j\omega) & 4\,\text{kHz} < f \le 28\,\text{kHz} \\ \dfrac{\varepsilon_{s2}}{1+(j2\pi fT_2)^{1-\nu_2}} & 28\,\text{kHz} < f \end{cases} \qquad (2)$$

where ν_1, ν_2 are the material parameters and ε^*_{s1} (the permittivity at zero frequency) is assumed to be a complex constant. It means that the ferrite beside of the magnetic hysteresis has also a ferroelectric one. The complex function $F(j\omega)$ must approximate decaying effect between both relaxation mechanisms occurring in this sample. It means that the $Ba_{0.25}Sr_{0.75}Fe_{12}O_{19}$ ferrite exhibits likely the static ferroelectric hysteresis loop, i.e. the sample has both the ferroelectric and ferrimagnetic properties. This fact has to be verified by an adequate and more precise experiment.

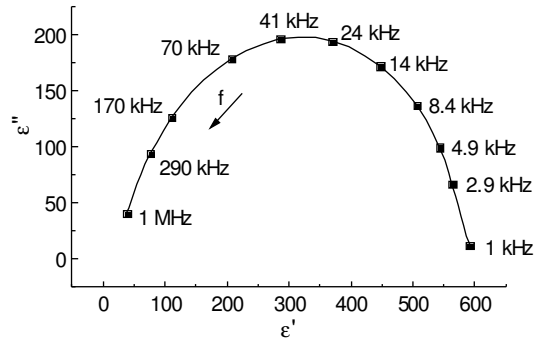

Fig. 5. Diagram of the complex permittivity for $Ba_{0.5}Sr_{0.5}Fe_{12}O_{19}$ at 67 °C (the parameter is frequency)

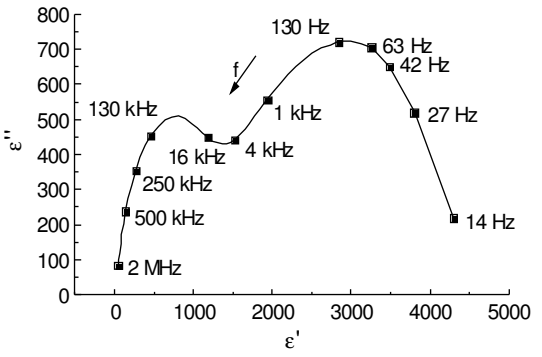

Fig. 6. Diagram of the complex permittivity for $Ba_{0.25}Sr_{0.75}Fe_{12}O_{19}$ at 66 °C (the parameter is frequency)

5. CONCLUSION

The strong decrease of ΔH_C occurring up to x = 0.3 for $(NiRu)_x$ and $(ZnRu)_x$ substitutions leads to conclusion that the anisotropy of $(NiRu)_x$ and $(ZnRu)_x$ becomes planar at small substitution. Observations of the $Ba_{1-y}Sr_yM$ ferrite samples has shown that T_C increases with ascending Sr concentration. The specific saturation polarization J_{s-m} is nearly independent on the Sr content, but ΔH_C slowly increases as the Sr content increases. However, ΔH_C decreases for $(BaSr)_{0.5}M$ hexaferrite when $2x$ Fe^{3+} cations are substituted by $(ZnTi)_x$. The $BaM(ZnTi)_x$ ferrite exhibits a higher decrease of ΔH_C for x<0.6. Probably for both cases the major role plays the substitution of Fe^{3+} ions with combination $(ZnTi)_x$ comparing with the substitution of Ba^{2+} with Sr^{2+} ions. The specific remanent polarization J_{s-r} decreases as x increased for both $BaM(ZnTi)_x$ and $(BaSr)_{0.5}M(ZnTi)_x$ ferrites. The dielectric properties of the measured $(BaSr)_{0.5}M$ ferrite are influenced by the relaxation effects. The frequency spectra of $\varepsilon^*(f)$ for $(Ba_{0.25}Sr_{0.75})M$ ferrite are determined by the relaxation and likely ferroelectric hysteresis effects. It means that $(Ba_{0.25}Sr_{0.75})M$ ferrite has probably the static ferroelectric hysteresis loops, i.e. this sample could be ferroelectric and ferrimagnetic at once. This fact must be experimental verified.

Acknowledgement

This work has been supported by both VEGA - Slovak Republic, under projects No. 1/3096/06, 1/4086/07 and EU/INTAS/07, and CONACyT – México.

REFERENCES

[1] Turilli, G. et al.: IEEE Trans. on Magn. 24, 1998, 2146.
[2] Han, D. H. et al.: J. Magn. Magn. Mat. 137, 1994, 191.
[3] Rane, M. V. et al.: J. Magn. Magn. Mat. 195, 1999, L 256
[4] Pignard, S. et al.: J. Magn. Magn. Mat. 260, 2003, 437
[5] The, G. B. et al.: Mat. Chem. and Phys. 101, 2007, 158.
[6] Grusková, A. et al.: J. Magn. Magn. Mater. 242–245, 2002, pp. 423
[7] González-Angeles, A. et al.: Mater. Lett. 59, 2005, pp. 26.
[8] González-Angeles, A. et al.: J. Magn. Magn. *Mater.* 285, 2005, pp. 450.
[9] González-Angeles, A. et al.: Mater. Lett. 59, 2005, pp. 1815
[10] Grusková, A. et al.: Acta Physica Polonica A, 113, 2008, pp. 1, 557
[11] Dosoudil, R.: J. El. Eng. 53, 2002, 10/S, 139.
[12] Grusková, A.: J. El. Eng. 53,2002, 10/S, 122.